Geophysical Research Letters

RESEARCH LETTER
10.1029/2022GL099793

Increasing Hurricane Intensification Rate Near the US Atlantic Coast

Karthik Balaguru[1], Gregory R. Foltz[2], L. Ruby Leung[1], Wenwei Xu[1], Dongmin Kim[2,3], Hosmay Lopez[2], and Robert West[2,4]

[1]Pacific Northwest National Laboratory, Richland, WA, USA, [2]NOAA/Atlantic Oceanographic and Meteorological Laboratory, Miami, FL, USA, [3]Cooperative Institute for Marine and Atmospheric Studies, University of Miami, Miami, FL, USA, [4]Northern Gulf Institute, Mississippi State University, Starkville, MS, USA

Key Points:

- Hurricane intensification rate has significantly increased near the US Atlantic coast over the last 40 years
- Climate models accurately simulate the observed trends with an enhanced environment conducive for hurricanes
- Multi-model projections suggest that the environment will increasingly favor hurricane intensification near the Atlantic coast

Supporting Information:

Supporting Information may be found in the online version of this article.

Correspondence to:

K. Balaguru,
Karthik.Balaguru@pnnl.gov

Citation:

Balaguru, K., Foltz, G. R., Leung, L. R., Xu, W., Kim, D., Lopez, H., & West, R. (2022). Increasing hurricane intensification rate near the US Atlantic coast. *Geophysical Research Letters*, *49*, e2022GL099793. https://doi.org/10.1029/2022GL099793

Received 27 MAY 2022
Accepted 28 JUL 2022

Abstract Hurricanes often cause severe damage and loss of life, and storms that intensify close to the coast pose a particularly serious threat. While changes in hurricane intensification and environment have been examined at basin scales previously, near-coastal changes have not been adequately explored. In this study, we address this using a suite of observations and climate model simulations. Over the 40-year period of 1979–2018, the mean 24-hr hurricane intensification rate increased by ~1.2 kt 6-hr^{-1} near the US Atlantic coast. However, a significant increase in intensification did not occur near the Gulf coast over the same period. The enhanced hurricane intensification along the Atlantic coast is consistent with an increasingly favorable dynamic and thermodynamic environment there, which is well simulated by climate models over the historical period. Further, multi-model projections suggest a continued enhancement of the storm environment and hurricane intensification near the Atlantic coast in the future.

Plain Language Summary While hurricanes pose a significant socioeconomic threat in general, those that intensify close to the coast are particularly challenging for operational forecasters and decision makers. Past studies examined basin-scale changes in hurricane intensification and the large-scale environment in the Atlantic. However, near-coastal changes in hurricane intensification have not been extensively studied. Herein, we address this using a combination of observations and numerical model simulations. Analysis of hurricane track data for the period 1979–2018 indicates that the mean hurricane intensification rate has increased significantly near the Atlantic coast. In contrast, significant increases in nearshore hurricane intensification are not seen for the Gulf coast. Observed changes in the ambient storm environment over the same period, which are in good agreement with these changes in hurricane intensification, are well reproduced by climate models. Finally, models project a continued enhancement of the hurricane environment near the Atlantic coast in the future. These results are well supported by direct simulation of hurricanes in high-resolution climate models.

1. Introduction

Hurricanes, and more generally tropical cyclones, are among the most destructive weather systems in tropical regions, with severe socioeconomic impacts worldwide (Klotzbach et al., 2018; Needham et al., 2015; Peduzzi et al., 2012). In the United States (US), individual hurricane events have historically been both the deadliest and costliest natural disasters (Grinsted et al., 2019; Rappaport, 2014; Wahl et al., 2015). With exposure of the population to hurricanes escalating at a far greater pace than to any other hazard (Iglesias et al., 2020), there are important implications for public health (Parks et al., 2021). Several previous studies have examined changes in various aspects of hurricanes that affect their impacts on land, such as their frequency, intensity, and translation speed (Balaguru et al., 2018; Bender et al., 2010; Bhatia et al., 2019; Elsner et al., 2008; Emanuel, 2005; Klotzbach et al., 2022; Knutson et al., 2020; Knutson et al., 2008; Kossin, 2018; L. Li & Chakraborty, 2020; Murakami et al., 2020; Patricola & Wehner, 2018; Sobel et al., 2016; Vecchi & Soden, 2007a; S. Wang et al., 2020; Webster et al., 2005; Zhu et al., 2021). However, most of these studies were conducted at basin or global scales, and few focused on the nearshore region.

When it comes to societal impacts, storms that intensify in the nearshore region pose a more serious threat (Emanuel, 2017), and represent a bigger challenge for damage mitigation, and consequently remain a high priority for operational forecasting. Using theory and numerical model simulations, Emanuel (2017) suggested that

hurricane intensification will likely increase under global warming, including in coastal regions. However, the analysis only considered rapid intensification and did not explore changes in the historical hurricane record. Kossin (2017) examined changes in hurricane intensification using observations focusing on the role of wind shear, though their analysis domain included much of the subtropical western Atlantic. Subsequently, Ting et al. (2019) examined the contributions of natural versus anthropogenic forcing to wind shear in the North Atlantic and how they may influence hurricane activity close to the US coast. They suggest, that under future greenhouse gas forcing, vertical wind shear will reduce considerably near the US Atlantic coast and will likely favor hurricane intensification over that region. Here, we build on these previous studies by examining changes in hurricane intensification more broadly in the important nearshore region. Our definition of nearshore includes the area within 200 nautical miles (~3°) of the coastline, which is the internationally accepted definition of "near-coastal" (United Nations, 1982). We attempt to understand the changes in hurricane intensification by considering the evolution of the large-scale environment and explore the likelihood that the observed changes in hurricane intensification will continue into the future.

2. Methods

2.1. Data

Hurricane track data based on the National Hurricane Center's HURDAT2 database are used to estimate hurricane track density and 24-hr intensification rates for the 40-year period 1979–2018. We obtain monthly mean sea surface temperature (SST), sea-level pressure, surface air temperature, surface pressure, winds, specific humidity, vertical velocity, and air temperature from the ECMWF Reanalysis version 5 (ERA5) (Hersbach et al., 2020) for the 40-year period 1979–2018 to understand changes in the hurricane environment (parameters include potential intensity (Emanuel, 1999), vertical wind shear evaluated between 200 and 850 hPa, relative vorticity at 850 hPa, and relative humidity at 600 hPa). To support our results based on ERA5, we performed a similar analysis of the hurricane environment using NCEP/NCAR atmospheric reanalysis (Kalnay et al., 1996) and Hadley SST data (Rayner et al., 2003). Daily rainfall data from the Global Historical Climatology Network (GHCN) (Menne et al., 2012) are combined with hurricane track data to estimate trends in hurricane-induced rainfall for the same 40-year period.

2.2. Models

Monthly mean output from 15 different fully coupled climate models belonging to the Coupled Model Intercomparison Project Phase 6 (CMIP6) (Eyring et al., 2016) are used to compute trends in the simulated hurricane environment over the historical period. Similarly, monthly mean data are obtained from 15 coupled climate models belonging to the Scenario Model Intercomparison Project (O'Neill et al., 2016) of CMIP6 to examine trends in the hurricane environment for the future period. More specifically, data is obtained for the "SSP585" scenario in which the planetary radiative forcing increases by 8.5 W m^{-2} by the year 2100. A description of various models used is provided in Tables S1 and S2 in Supporting Information S1. Hurricane track data are obtained from five fully coupled models belonging to the High Resolution Model Intercomparison Project (HighResMIP) of CMIP6 (R. J. Haarsma et al., 2016). The atmospheric component of the selected models has a resolution of approximately 50 km or higher, allowing for explicit simulation of hurricanes (M. J. Roberts et al., 2020). We obtain tracks generated using TempestExtremes, a scale-aware feature tracking software that operates on the model native grid (Ullrich et al., 2021). These track data (M. Roberts, 2019) are used to explore changes in simulated hurricane intensification rates. A description of various HighResMIP models used is provided in Table S3 in Supporting Information S1.

2.3. Calculations

The hurricane track density is obtained by binning 6-hr hurricane track locations into 5° by 5° bins. Only storm locations where the maximum sustained wind speed is 35 kt or higher are included in the track density estimates. The raw hurricane track density fields were smoothed spatially using a nine-point moving average weighted by the distance from the center (Murakami et al., 2020; B. Wang et al., 2010). We select rain gauges belonging to GHCN that have complete recordings of daily rainfall since 1979 and are within 2° of the US Atlantic and Gulf coasts. Observed hurricane tracks from 1979 to 2018 are then used to extract hurricane-induced precipitation. A

daily rainfall recording is considered to be hurricane-induced if an observed hurricane track passes within 500 km of the gauge during that day. The identified data are then aggregated over the year to get the annual cumulative hurricane-induced rainfall at each gauge location. If no hurricane passes within 500 km of a particular gauge during a year, the value is recorded as zero for that year. Significance of monotonic upward or downward trends in track density and rainfall is evaluated using the non-parametric Mann–Kendall test (Gilbert, 1987).

The 24-hr intensification rate is estimated as the linear regression coefficient of the maximum wind speed over five successive 6-hourly track locations, including the current location. All locations where the initial storm intensity is at least tropical storm strength (35 kt) are included in the computation of intensification rate. Further, the data is sub-sampled to ensure that the distributions of initial storm state (initial maximum wind speed and translation speed) are statistically similar over the two 20-year periods (1979–1998 and 1999–2018). More specifically, a minimum translation speed of 3.5 m s^{-1} is used to sub-sample data. Points where the storm crosses over land during this 24-hr period are not considered. In addition, we exclude points within 0.5° of the US coast to further reduce land effects.

Similar methods are used to calculate 24-hr intensification rates for the HighResMIP models. Data are pooled together from the different models before calculating the mean intensification rate for each period. As in observations, the data are subsampled to ensure that the results are independent of the initial storm state. The Monte Carlo method of repeated random sampling is employed to generate error bars for the probability distribution functions (PDFs). From a given distribution, we randomly select half of the data points to generate a PDF. This process is then repeated 1,000 times. Subsequently, the mean and standard deviation computed across the various PDFs yield the mean PDF and error bar magnitudes, respectively. The vertical moisture flux convergence is estimated as $-\frac{\partial(w\,q)}{\partial p}$ where w is the vertical velocity (Pa s^{-1}), q is the specific humidity (kg kg^{-1}) and p is the pressure (Pa).

3. Results

3.1. Observed Changes in Nearshore Hurricane Intensification

We begin by examining the Atlantic hurricane database (C. W. Landsea & Franklin, 2013) over the 40-year satellite period of 1979–2018, when the record is most reliable. Trends in hurricane track density are positive over much of the basin (Figure 1a), and the spatial pattern is broadly consistent with Murakami et al. (2020). Areas of significant positive trends include the hurricane main development region between 80°W and 20°W and 10°N–20°N, and the tropical and subtropical Atlantic to the west of 40°W. Interestingly, significant positive trends are found near the Atlantic coast while trends are insignificant near the Gulf coast. This difference in trends between the Atlantic and Gulf coasts, which is also seen in Murakami et al. (2020), suggests an increasing preference for hurricanes to be found in the western Atlantic and closer to the US coast, particularly off of the eastern seaboard. One of the major impacts of landfalling hurricanes is freshwater flooding from excessive rainfall (Knutson et al., 2020; Kunkel et al., 2010). An evaluation of 40-year changes in hurricane-induced rainfall based on rain gauge data (Figure 1b) shows that there are significant positive trends, especially near the mid-to-upper Atlantic coast and portions of the southeastern US over Florida. These trends in precipitation from hurricanes are also consistent with the idea that hurricane activity has increased near the Atlantic coast (Figure 1a; Murakami et al. (2020)). However, while track density can be a useful indicator of hurricane activity, it can be influenced by non-local factors such as frequency (Emanuel, 2021) and steering flow (S. Wang & Toumi, 2021). Hence, we next consider the intensification rate, a more direct metric of local changes in hurricanes.

The probability distributions of 24-hr hurricane intensification rates for the Atlantic and Gulf coasts are examined for the two 20-year periods 1979–1998 and 1999–2018. We consider the months of June–October during which more than 98% of US hurricane landfalls have occurred. Figures 1c and 1e indicate the track locations considered for this analysis. Relative to the earlier period, the distribution of intensification rates is noticeably shifted toward more positive values in the later period for the Atlantic coast (Figure 1d). The mean intensification rate for 1979–1998 was −1.21 kt 6-hr^{-1}, and it increased to −0.01 kt 6-hr^{-1} during 1999–2018, a difference that is significant at the 95% level. In contrast, the mean intensification rate did not increase significantly near the Gulf coast; the intensification rates are 1.71 kt 6-hr^{-1} and 2.47 kt 6-hr^{-1} for the earlier and later periods, respectively (Figure 1f). However, note that instances of rapid intensification (intensification rate ≥7.5 kt 6-hr^{-1}) appear to have increased for both regions, consistent with previous studies (Bhatia et al., 2019). The increase in the mean hurricane intensification rate near the Atlantic coast noted above gets stronger as we approach the coast and

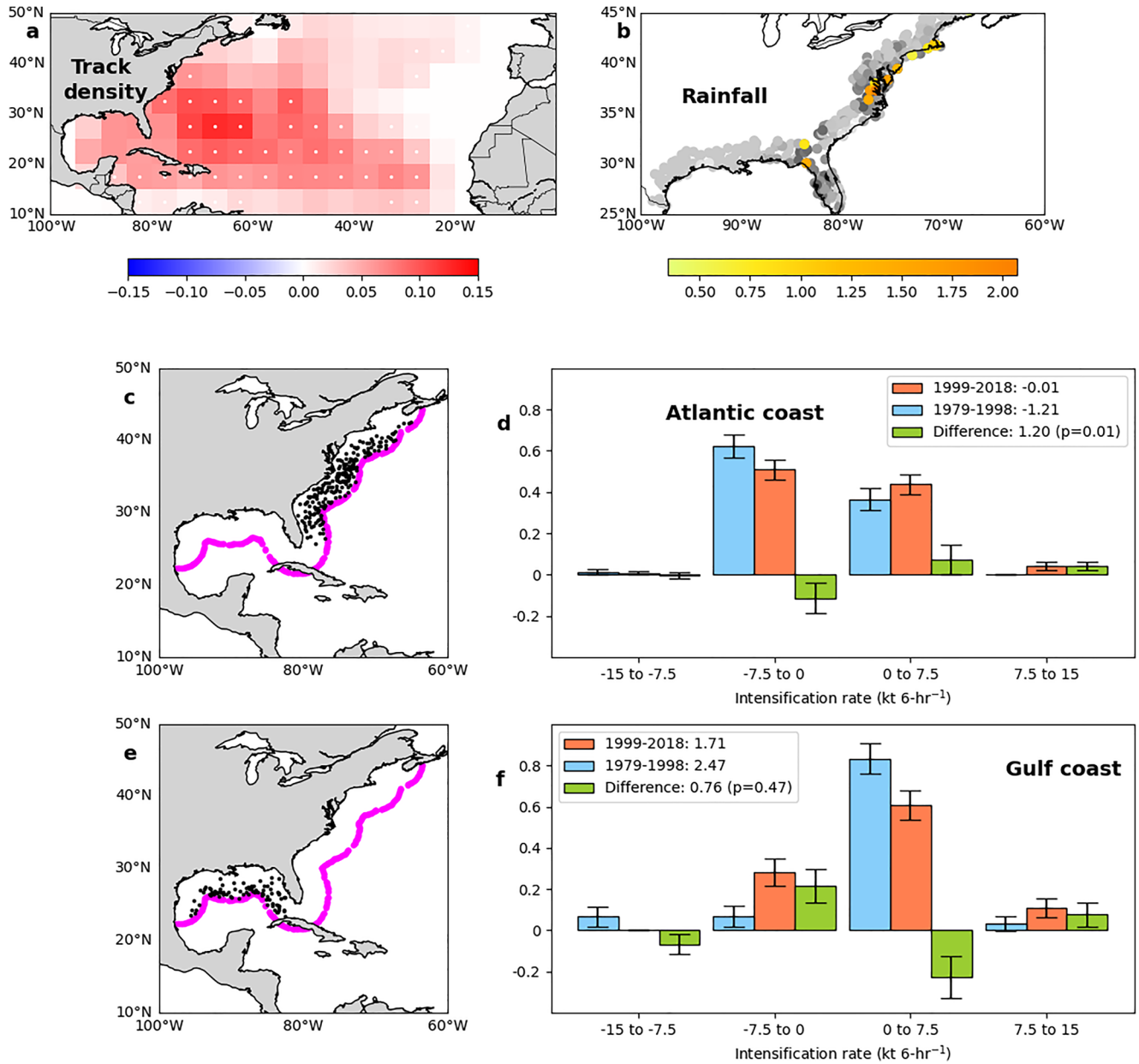

Figure 1. Observed changes in near-coastal hurricanes (1979–2018). (a) Trends in June–November hurricane track density using 6-hr track locations where the wind speed is 35 kt or higher. White dots represent locations where the trends are statistically significant at the 95% level based on a Mann–Kendall test. (b) Trends in accumulated rainfall from hurricanes (mm year^{-1}). Values shaded in yellow-orange are significant at the 95% level based on a Mann–Kendall test. Values shaded in gray represent locations where the trends are insignificant. Nearshore Atlantic hurricane track locations (black dots) within ∼3° of the US (c) Atlantic coast and (e) Gulf coast. Probability distributions of 24-hr intensification rates for the periods 1979–1998 (blue), 1999–2018 (orange), and their difference (green) based on locations that are within ∼3° of the US (d) Atlantic coast and (f) Gulf coast. The error bars in panels d and f representing the standard deviation of the distribution are generated based on the Monte Carlo technique. The mean intensification rates for each period, their difference and the *p*-value for statistical significance (based on a Student's *t*-test) are shown in the legend for panels d and f.

weakens away from the coast (Figure S1 in Supporting Information S1), highlighting the regional nature of the signal and indicating that it is not part of a broader basin-wide change. In addition, these trends in near-coastal intensification rates are insensitive to the exact period chosen (Figure S2 in Supporting Information S1) and are consistent with those in track density shown earlier, prompting us to ask the following question: What changes in the storm environment caused the observed enhancement in near-coastal Atlantic hurricane activity?

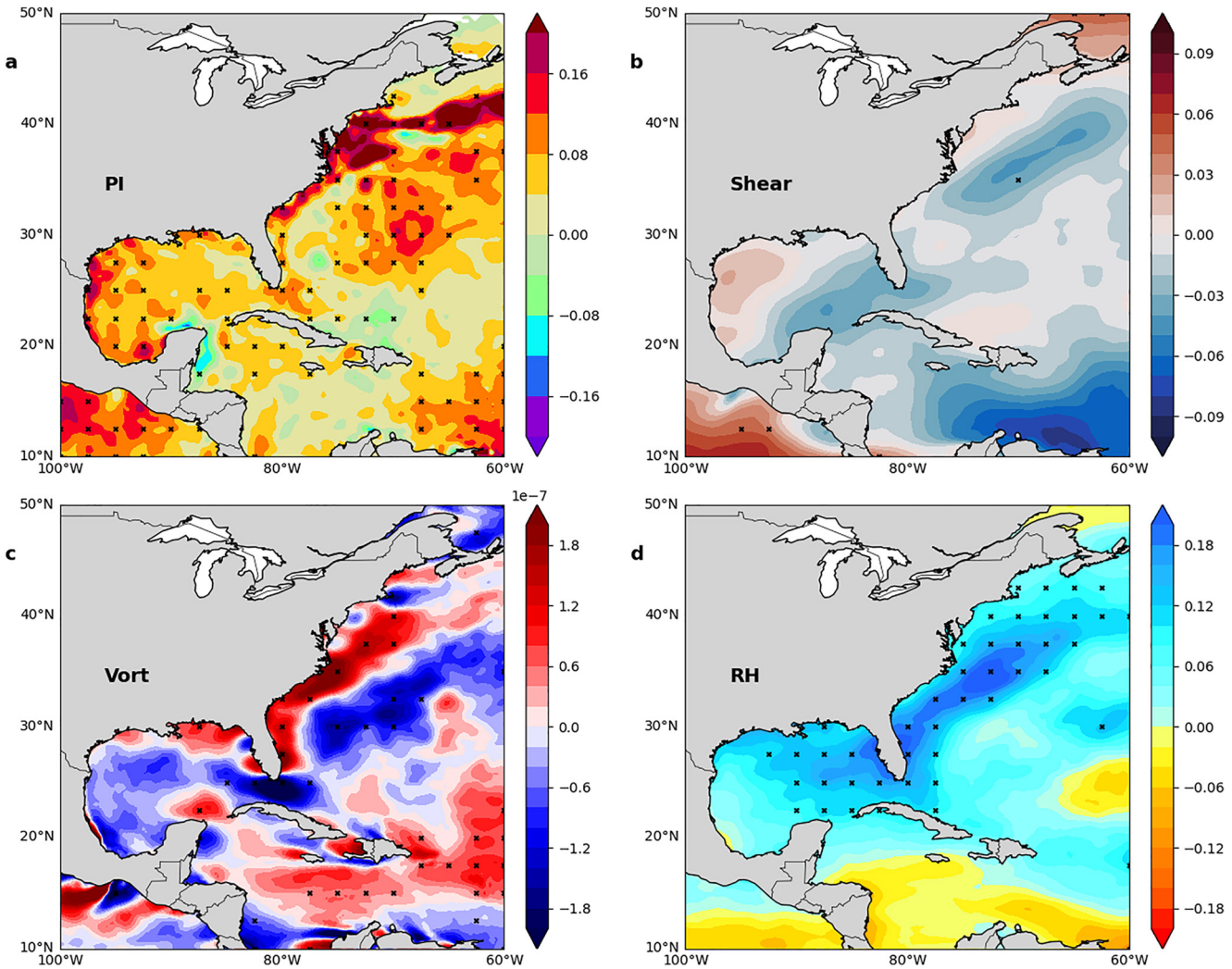

Figure 2. Observed changes in the nearshore hurricane environment (1979–2018). 40-Year trends in (a) potential intensity (ms^{-1} $year^{-1}$), (b) vertical wind shear (ms^{-1} $year^{-1}$), (c) relative vorticity at 850 hPa (s^{-1} $year^{-1}$), and (d) relative humidity at 600 hPa (% $year^{-1}$) based on ERA5 reanalysis and averaged over the months of June–October. Black crosses in various panels represent locations where the trends are statistically significant at the 95% level based on a Student's *t*-test.

3.2. Change in the Nearshore Hurricane Environment

We now examine changes in the large-scale ocean-atmosphere environment relevant for hurricane development over the period 1979–2018. Forty-year ERA5 (Hersbach et al., 2020) trends in various dynamical and thermodynamic variables critical to hurricane intensification (DeMaria et al., 2005) suggest an increasingly favorable environment for hurricanes near the Atlantic coast (Figure 2). Significant positive trends are found in potential intensity (Emanuel, 1999) over a broad area of the western Atlantic, with the strongest trends occurring in the northwestern Atlantic near the US coast (Figure 2a). While vertical wind shear (evaluated between 200 and 850 hPa) has decreased off of the Atlantic coast (Figure 2b), trends in wind shear are mixed for the Gulf coast, with decreases in the eastern Gulf of Mexico and increases in the western Gulf of Mexico. Strong positive trends in lower-tropospheric relative vorticity (evaluated at 850 hPa) are found near the Atlantic coast (Figure 2c), while trends in low-level vorticity are mostly negative in the Gulf of Mexico except for a small region near the coasts of Mississippi and Alabama. Trends in mid-tropospheric relative humidity (evaluated at 600 hPa) are strongly positive near the Atlantic coast (Figure 2d). Albeit with a weaker magnitude, trends in humidity are also positive in the Gulf of Mexico with the strongest trends occurring in the eastern part of the region and decreasing westwards. Taken together, these results suggest that the nearshore environment has become more favorable for hurricanes near the Atlantic coast, consistent with the observed increase in the intensification of hurricanes in

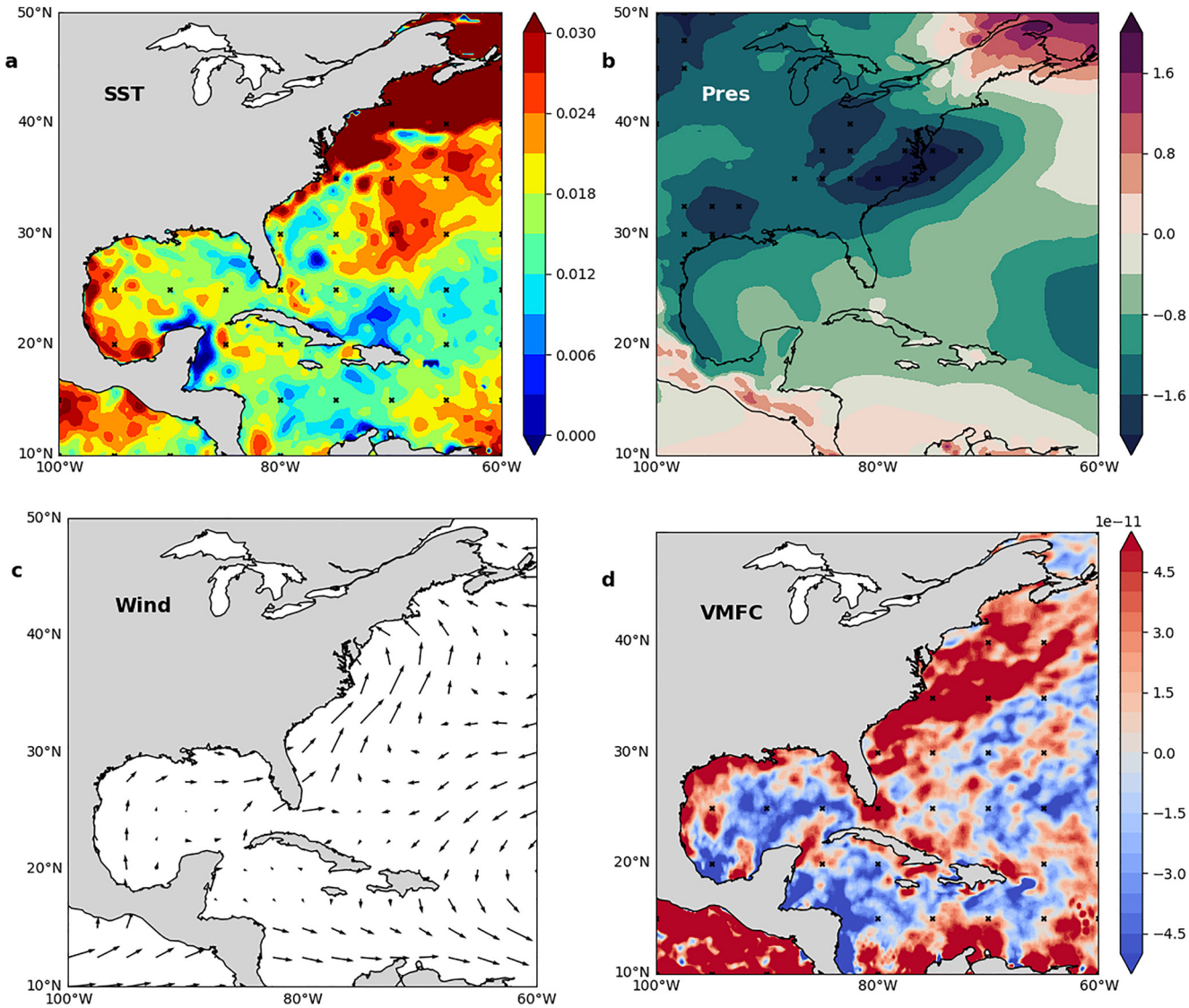

Figure 3. Understanding changes in the nearshore hurricane environment (1979–2018). 40-Year trends in (a) SST (°C year^{-1}), (b) surface pressure (Pa year^{-1}), (c) circulation at 850 hPa (ms^{-1} year^{-1}), and (d) vertical moisture flux convergence (s^{-1} year^{-1}) at 600 hPa, based on ERA5 reanalysis and averaged over the months of June–October. Black crosses in various panels represent locations where the trends are statistically significant at the 95% level based on a Student's *t*-test.

that region. For the Gulf coast however, while trends in potential intensity and mid-level humidity are favorable for hurricanes, changes in vertical wind shear and low-level vorticity are mixed and less favorable.

To further understand these environmental changes, we next consider trends in SST. The increase in potential intensity near the US coast is likely due to SST warming over the northwestern Atlantic (Figure 3a), which has been attributed in part to a slowdown of the Atlantic Meridional Overturning Circulation and the associated retreat of the Labrador Sea Current (Saba et al., 2016). The spatial pattern of SST warming is also consistent with an enhanced summer North Atlantic subtropical high (W. Li et al., 2012; Ting et al., 2015). The decrease in vertical wind shear off of the Atlantic coast and over the eastern Gulf of Mexico is potentially a consequence of global warming (Camargo, 2013; Kossin, 2017; Ting et al., 2019; Vecchi & Soden, 2007b), a point we will return to later in the paper. To understand changes in low-level vorticity, consider trends in surface pressure (Figure 3b) and winds at 850 hPa (Figure 3c). A pressure gradient across the land-sea boundary develops during this period, with strong decreases in surface pressure near the mid-Atlantic coast. This triggers the formation of an anomalous low-level cyclonic circulation (Figure 3c) that can directly increase low-level vorticity near the coast. Further, the enhanced low-level vorticity can increase mid-tropospheric relative humidity through an increase in vertical

moisture flux convergence (Figure 3d). Note that the observed SST warming in the western Atlantic can also contribute to positive trends in humidity. While these results are based on ERA5 reanalysis, similar results were obtained using NCEP/NCAR reanalysis (Kalnay et al., 1996) and Hadley SST (Rayner et al., 2003), underlining their robustness (Figure S3 in Supporting Information S1).

So far, we have seen that nearshore hurricane intensification has increased significantly, with conspiring changes in the large-scale hurricane environment. This raises the question of whether these environmental changes are caused by natural variability in the climate system or if there is a role for climate change. To address this, we use simulations of the large-scale environment from fully coupled climate models belonging to CMIP6 (Eyring et al., 2016) to examine the relevance of internal variability versus external forcing. Over the historical period of 1980–2014, trends near the Atlantic coast are strongly positive for potential intensity (Figure S4a in Supporting Information S1) and low-level relative vorticity (Figure S4c in Supporting Information S1), and strongly negative for wind shear (Figure S4b in Supporting Information S1). For the Gulf coast, though trends in wind shear are negative, changes in potential intensity and low-level vorticity are less favorable. Trends in mid-tropospheric humidity (Figure S4d in Supporting Information S1), which are positive near the Gulf coast and weakly positive near the Atlantic coast, agree less with those from observations (Figure 2d), suggesting that natural variability may partly be responsible for the observed trends in humidity. Despite this, the CMIP6 multi-model ensemble mean is broadly consistent with observations and reveals an increasingly favorable hurricane environment near the Atlantic coast.

As in observations, simulated trends in potential intensity closely follow those in SST, with the strongest surface warming occurring in the northwestern Atlantic (Figure S5a in Supporting Information S1). The models also simulate the development of the surface pressure gradient across the land-sea boundary with an anomalous low-pressure area over the mid-Atlantic coast (Figure S5b in Supporting Information S1). This leads to the formation of a low-level cyclonic circulation anomaly (Figure S5c in Supporting Information S1) that enhances lower-tropospheric relative vorticity near the Atlantic coast. Finally, trends in mid-level relative humidity may be due to a combination of SST warming and an increase in vertical moisture flux convergence (Figure S5d in Supporting Information S1). The presence of the observed signal in the multi-model ensemble mean of CMIP6 suggests that the changes occurring in nearshore Atlantic hurricane activity are due in part to external forcing, as internal variability is largely suppressed by averaging across the multi-model simulations.

3.3. Future Projections of Nearshore Hurricane Environment

To determine whether ongoing changes in hurricanes and their large-scale environment might continue into the future, and to more clearly understand the role of external forcing, we analyzed CMIP6 models under the "SSP585" emissions scenario, which represents a fossil-based world economy that is hurtling toward an increase in planetary radiative forcing of 8.5 W m^{-2} by 2100. Trends for the 86-year period 2015–2100 indicate that the nearshore environment will continue to become more favorable for hurricane intensification near the Atlantic coast (Figure 4). Positive trends are found for potential intensity near the Atlantic coast as well as the Gulf coast (Figure 4a). This projected increase in potential intensity near the coastal regions has also been noted in previous studies (Camargo, 2013; Camargo et al., 2013; Sobel et al., 2016; Ting et al., 2015; Vecchi & Soden, 2007b). Negative trends in vertical wind shear are obtained near the northeastern Gulf of Mexico, but shear decreases more broadly and strongly near the Atlantic coast (Figure 4b). While observed trends in vertical wind shear were weakly negative (Figure 2b), the multi-model mean produces a stronger and more significant decrease in shear for both the historical period (Figure S2b in Supporting Information S1) as well as future projections near the Atlantic coast (Figure 4b). This likely suggests that the weaker decrease in shear in observations is due to competing effects of natural variability and external forcing, and it is in good agreement with previous studies (Camargo, 2013; Kossin, 2017; Ting et al., 2019; Vecchi & Soden, 2007b) that suggest that external forcing tends to decrease vertical wind shear near the US Atlantic coast. While trends in low-level relative vorticity are positive near the Atlantic coast to the north of 30°N (Figure 4c), they are predominantly negative and less favorable for hurricanes in the Gulf of Mexico and near eastern Florida. Mid-tropospheric relative humidity increases near the Atlantic coast, with the strongest trends occurring near the mid-Atlantic region. In the Gulf of Mexico, positive trends in humidity to the north are compensated by decreases to the south. As in observations and multi-model simulations for the historical period, these projected changes in the environment are driven by strong sea surface warming (Figure S6a in Supporting Information S1), development of a pressure gradient across the land-sea

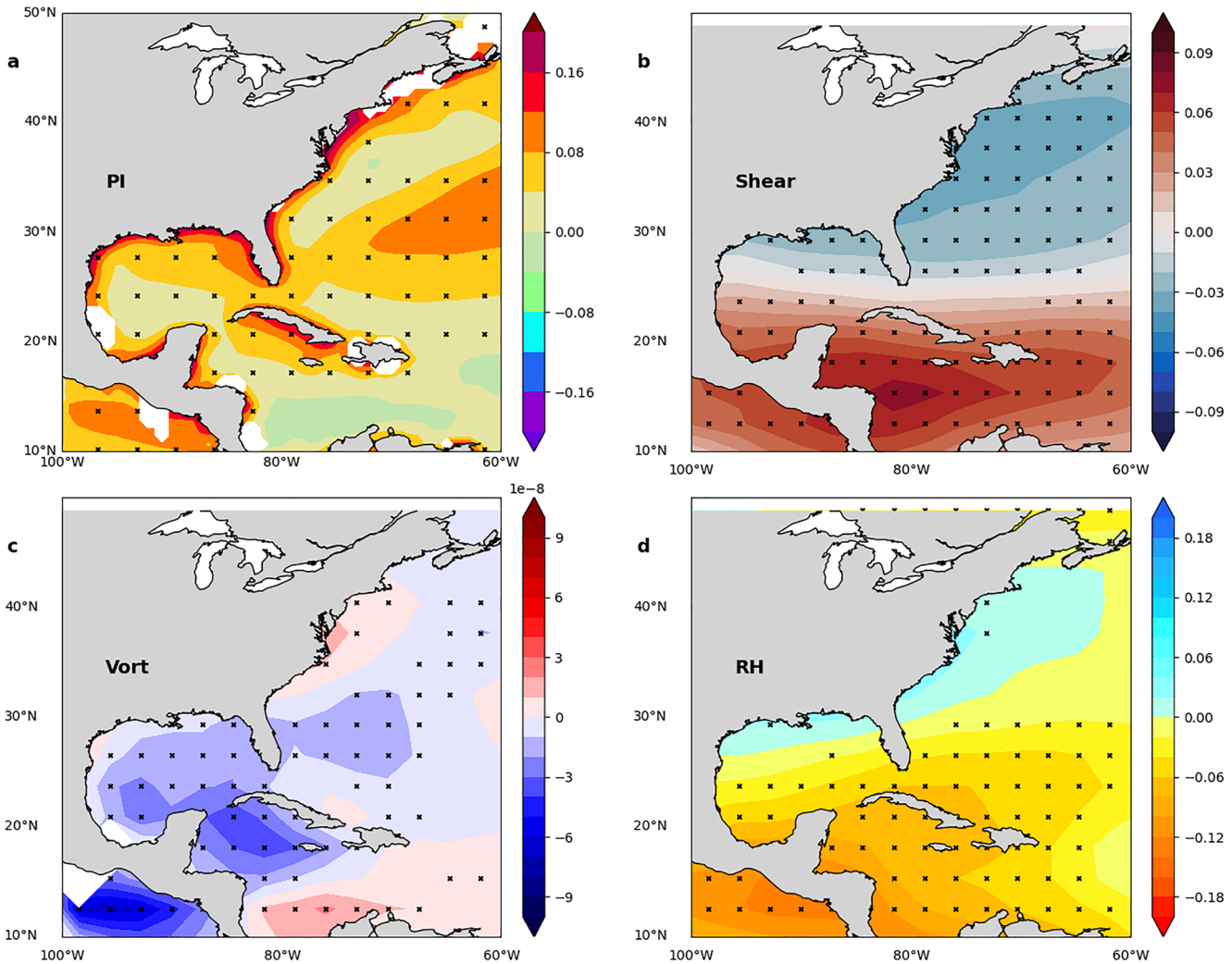

Figure 4. Projected changes in the nearshore hurricane environment (2015–2100). Multi-model ensemble mean trends in (a) potential intensity (ms^{-1} $year^{-1}$), (b) vertical wind shear (ms^{-1} $year^{-1}$), (c) relative vorticity at 850 hPa (s^{-1} $year^{-1}$), and (d) relative humidity at 600 hPa (% $year^{-1}$), based on 15 CMIP6 climate models. Trends are computed over the 86-year period 2015–2100 based on the "SSP585" emissions scenario. All variables are averaged during June–October. Crosses represent locations where at least 11 out of the 15 models agree on the sign of the trend.

boundary (Figure S6b in Supporting Information S1), and an associated low-level cyclonic circulation anomaly (Figure S6c in Supporting Information S1). There is also an increase in vertical moisture flux convergence (Figure S6d in Supporting Information S1).

Finally, we also analyzed direct simulations of hurricanes from HighResMIP (R. J. Haarsma et al., 2016) to further assess the robustness of these results (Figure S7 in Supporting Information S1). While the nominal resolution of the atmospheric component of models is about 1° in CMIP6, it increases to as much as 0.25° in HighResMIP, thereby allowing explicit simulation of hurricanes (M. J. Roberts et al., 2020). For the 72-year period 1979–2050, the HighResMIP multi-model ensemble projects an increase in the mean 24-hr intensification rate of 0.35 kt 6-hr^{-1} for the Atlantic coast, a value significant at the 95% level. For the Gulf coast, the change in the mean hurricane intensification rate is insignificant. These results are consistent with the observed changes in hurricane intensification over the historical period and are in broad agreement with projected changes in the hurricane environment.

4. Discussion

Using observations and ensembles of fully coupled climate model simulations, we demonstrated that the magnitude of hurricane intensification has been increasing near the US Atlantic coast. Multi-model means of historical simulations and future climate simulations with external forcing show changes in the near-coastal environment that are broadly consistent with the observed changes. Over the historical period, observations (Figure 3b) show an increase in pressure gradient across the land-sea boundary, especially along the US Atlantic coast. Albeit with a slightly different spatial pattern, an increase in pressure gradient across the land-sea boundary is also simulated in future projections of the large-scale environment (Figure S6b in Supporting Information S1). This enhancement of the pressure gradient across the land-sea boundary is linked to an increase in the lower-level cyclonic circulation and vorticity along the Atlantic coast. While a decrease in pressure over land is mainly responsible for the increase in the land-sea pressure gradient over the historical period, an increase in pressure over the ocean (W. Li et al., 2012) may also play a role in the future. We speculate that the decreases in pressure over land may be related to an increase in the land-sea warming contrast (Figure S8 in Supporting Information S1), which is a robust response to external forcing (Sutton et al., 2007). However, besides external forcing, internal variability may also play a role (Camargo, 2013), as the observed changes in the hurricane environment are noticeably larger compared to the simulated changes driven by external forcing. More studies using sensitivity experiments are needed to clearly delineate the relative contributions of external forcing and natural variability to the change in the hurricane environment, including the potential role of an evolving land-sea warming contrast.

Based on observed and simulated changes in potential intensity and wind shear, Ting et al. (2019) suggested that hurricanes may intensify more strongly near the Atlantic coast and more slowly near the Gulf coast in the future. Based on climate model projections of the ventilation index, Tang and Camargo (2014) also suggested that the large-scale environment will become less favorable near the Gulf coast relative to the Atlantic coast. We present evidence for this using historical hurricane track data and direct simulations of hurricanes from HighResMIP. Further, we show that besides wind shear, factors such as low-level relative vorticity may also contribute to the contrasting changes in hurricane intensification near the Atlantic and Gulf coasts. These findings have profound implications for policy- and decision-makers and inhabitants of coastal areas. Previously, changes in the characteristics of hurricanes, such as decreases in translation speed (Kossin, 2018) and decay rate after landfall (L. Li & Chakraborty, 2020), have been suggested as potential reasons for an increase in hurricane-induced freshwater flooding. In this study, we show that hurricanes are entering an increasingly favorable environment near the US Atlantic coast just ahead of landfall, a process that can further exacerbate those effects.

In this study, we focused on changes in nearshore Atlantic hurricane intensification over the historical period and examined whether they may continue into the future. However, some previous studies noted an intensification of landfalling tropical cyclones in other regions, such as in the western Pacific (Mei & Xie, 2016). Therefore, one wonders whether the mechanism identified in this study may also manifest in other regions affected by tropical cyclones. To address this, we performed a similar analysis for the other Northern Hemisphere tropical cyclone basins under the "SSP585" scenario (Figure S9 in Supporting Information S1). Under this strong external forcing, significant warming over land will continue (Figure S9a in Supporting Information S1). In response, low-pressure areas with cyclonic circulations approximately straddling the land-sea boundaries also develop near the coastal regions of the Northwest Pacific and the northern Arabian Sea (Figure S9b in Supporting Information S1). Associated with these circulation anomalies are areas of enhanced positive vorticity near the coast (Figure S9c in Supporting Information S1). This finding underlines the broad nature of our results and points to their relevance for other regions in the global tropics vulnerable to tropical cyclones.

Data Availability Statement

The sources for various observational data used in this study are as follows: Hurricane track data (https://www.nhc.noaa.gov/data/%23hurdat), ERA5 reanalysis data (https://www.ecmwf.int/en/forecasts/datasets/reanalysis-datasets/era5), NCEP/NCAR reanalysis data (https://psl.noaa.gov/data/gridded/data.ncep.reanalysis.html), Hadley SST data (https://www.metoffice.gov.uk/hadobs/hadisst/), Daily rainfall from GHCN (https://www.ncei.noaa.gov/products/land-based-station/global-historical-climatology-network-daily), CMIP6 data for the historical period (https://esgf-node.llnl.gov/projects/cmip6/), CMIP6 data under the "SSP585" scenario

(https://esgf-node.llnl.gov/projects/cmip6/), and HighResMIP hurricane track data (https://data.ceda.ac.uk/badc/highresmip-derived/data/storm_tracks/TempExt).

Acknowledgments
K. B., L. R. L., and W. X. are supported by the Office of Science (BER) of the U.S. Department of Energy as part of the Regional and Global Model Analysis (RGMA) program area through the Water Cycle and Climate Extremes Modeling project and the collaborative multi-program Integrated Coastal Modeling project. The Pacific Northwest National Laboratory is operated for DOE by the Battelle Memorial Institute under contract DE-AC05-76RL01830. G. R. F. was funded by base funds to NOAA/AOML's Physical Oceanography Division. The computations were mainly carried out using the computing resources at the National Energy Research Scientific Computing Center (NERSC), a U.S. Department of Energy Office of Science User Facility located at Lawrence Berkeley National Laboratory, operated under Contract No. DE-AC02-05CH11231. We acknowledge the World Climate Research Programme, which, through its Working Group on Coupled Modelling, coordinated and promoted CMIP6. We thank the climate modeling groups for producing and making available their model output, the Earth System Grid Federation (ESGF) for archiving the data and providing access, and the multiple funding agencies who support CMIP6 and ESGF. We thank DOE's RGMA program area, the Data Management program, and NERSC for making this coordinated CMIP6 analysis activity possible.

References

Balaguru, K., Foltz, G. R., & Leung, L. R. (2018). Increasing magnitude of hurricane rapid intensification in the central and eastern tropical Atlantic. *Geophysical Research Letters*, *45*(9), 4238–4247. https://doi.org/10.1029/2018GL077597

Bender, M. A., Knutson, T. R., Tuleya, R. E., Sirutis, J. J., Vecchi, G. A., Garner, S. T., & Held, I. M. (2010). Modeled impact of anthropogenic warming on the frequency of intense Atlantic hurricanes. *Science*, *327*(5964), 454–458. https://doi.org/10.1126/science.1180568

Bhatia, K. T., Vecchi, G. A., Knutson, T. R., Murakami, H., Kossin, J., Dixon, K. W., & Whitlock, C. E. (2019). Recent increases in tropical cyclone intensification rates. *Nature Communications*, *10*(1), 1–9. https://doi.org/10.1038/s41467-019-08471-z

Camargo, S. J. (2013). Global and regional aspects of tropical cyclone activity in the CMIP5 models. *Journal of Climate*, *26*(24), 9880–9902. https://doi.org/10.1175/JCLI-D-12-00549.1

Camargo, S. J., Ting, M., & Kushnir, Y. (2013). Influence of local and remote SST on North Atlantic tropical cyclone potential intensity. *Climate Dynamics*, *40*(5), 1515–1529. https://doi.org/10.1007/s00382-012-1536-4

De Maria, M., Mainelli, M., Shay, L. K., Knaff, J. A., & Kaplan, J. (2005). Further improvements to the statistical hurricane intensity prediction scheme (SHIPS). *Weather and Forecasting*, *20*(4), 531–543. https://doi.org/10.1175/WAF862.1

Elsner, J. B., Kossin, J. P., & Jagger, T. H. (2008). The increasing intensity of the strongest tropical cyclones. *Nature*, *455*(7209), 92–95. https://doi.org/10.1038/nature07234

Emanuel, K. A. (1999). Thermodynamic control of hurricane intensity. *Nature*, *401*(6754), 665–669. https://doi.org/10.1038/44326

Emanuel, K. A. (2005). Increasing destructiveness of tropical cyclones over the past 30 years. *Nature*, *436*(7051), 686–688. https://doi.org/10.1038/nature03906

Emanuel, K. A. (2017). Will global warming make hurricane forecasting more difficult? *Bulletin of the American Meteorological Society*, *98*(3), 495–501. https://doi.org/10.1175/BAMS-D-16-0134.1

Emanuel, K. A. (2021). Atlantic tropical cyclones downscaled from climate reanalyses show increasing activity over past 150 years. *Nature Communications*, *12*(1), 7027. https://doi.org/10.1038/s41467-021-27364-8

Eyring, V., Bony, S., Meehl, G. A., Senior, C. A., Stevens, B., Stouffer, R. J., & Taylor, K. E. (2016). Overview of the Coupled Model Intercomparison Project Phase 6 (CMIP6) experimental design and organization. *Geoscientific Model Development*, *9*(5), 1937–1958. https://doi.org/10.5194/gmd-9-1937-2016

Gilbert, R. O. (1987). *Statistical methods for environmental pollution monitoring*. John Wiley & Sons.

Grinsted, A., Ditlevsen, P., & Christensen, J. H. (2019). Normalized US hurricane damage estimates using area of total destruction, 1900–2018. *Proceedings of the National Academy of Sciences*, *116*(48), 23942–23946. https://doi.org/10.1073/pnas.1912277116

Haarsma, R. J., Roberts, M. J., Vidale, P. L., Senior, C. A., Bellucci, A., Bao, Q., et al. (2016). High Resolution Model Intercomparison Project (HighResMIP v1.0) for CMIP6. *Geoscientific Model Development*, *9*(11), 4185–4208. https://doi.org/10.5194/gmd-9-4185-2016

Hersbach, H., Bell, B., Berrisford, P., Hirahara, S., Horányi, A., Muñoz-Sabater, J., et al. (2020). The ERA5 global reanalysis. *Quarterly Journal of the Royal Meteorological Society*, *146*(730), 1999–2049. https://doi.org/10.1002/qj.3803

Iglesias, V., Braswell, A. E., Rossi, M. W., Joseph, M. B., McShane, C., Cattau, M., et al. (2020). Risky development: Increasing exposure to natural hazards in the United States. *Earth's Future*, *9*(7), e2020EF001795. https://doi.org/10.1029/2020EF001795

Kalnay, E., Kanamitsu, M., Kistler, R., Collins, W., Deaven, D., Gandin, L., et al. (1996). The NCEP/NCAR 40-year reanalysis project. *Bulletin of the American Meteorological Society*, *77*(3), 437–472. https://doi.org/10.1175/1520-0477(1996)077<0437:TNYRP>2.0.CO;2

Klotzbach, P. J., Bowen, S. G., Pielke, R., & Bell, M. (2018). Continental U.S. hurricane landfall frequency and associated damage: Observations and future risks. *Bulletin of the American Meteorological Society*, *99*(7), 1359–1376. https://doi.org/10.1175/BAMS-D-17-0184.1

Klotzbach, P. J., Wood, K. M., Schreck, C. J., III, Bowen, S. G., Patricola, C. M., & Bell, M. M. (2022). Trends in global tropical cyclone activity: 1990–2021. *Geophysical Research Letters*, *49*(6), e2021GL095774. https://doi.org/10.1029/2021GL095774

Knutson, T., Camargo, S. J., Chan, J. C., Emanuel, K. A., Ho, C.-H., Kossin, J., et al. (2020). Tropical cyclones and climate change assessment: Part II: Projected response to anthropogenic warming. *Bulletin of the American Meteorological Society*, *101*(3), E303–E322. https://doi.org/10.1175/BAMS-D-18-0194.1

Knutson, T. R., Sirutis, J. J., Garner, S. T., Vecchi, G. A., & Held, I. M. (2008). Simulated reduction in Atlantic hurricane frequency under twenty-first-century warming conditions. *Nature Geoscience*, *1*(6), 359–364. https://doi.org/10.1038/nheo202

Kossin, J. P. (2017). Hurricane intensification along United States coast suppressed during active hurricane periods. *Nature*, *541*(7637), 390–393. https://doi.org/10.1038/nature20783

Kossin, J. P. (2018). A global slowdown of tropical-cyclone translation speed. *Nature*, *558*(7708), 104–107. https://doi.org/10.1038/s41586-018-0158-3

Kunkel, K. E., Easterling, D. R., Kristovich, D. A., Gleason, B., Stoecker, L., & Smith, R. (2010). Recent increases in US heavy precipitation associated with tropical cyclones. *Geophysical Research Letters*, *37*(24). https://doi.org/10.1029/2010GL045164

Landsea, C. W., & Franklin, J. L. (2013). Atlantic hurricane database uncertainty and presentation of a new database format. *Monthly Weather Review*, *141*(10), 3576–3592. https://doi.org/10.1175/MWR-D-12-00254.1

Li, L., & Chakraborty, P. (2020). Slower decay of landfalling hurricanes in a warming world. *Nature*, *587*(7833), 230–234. https://doi.org/10.1038/s41586-020-2867-7

Li, W., Li, L., Ting, M., & Liu, Y. (2012). Intensification of Northern Hemisphere subtropical highs in a warming climate. *Nature Geoscience*, *5*(11), 830–834. https://doi.org/10.1038/ngeo1590

Mei, W., & Xie, S.-P. (2016). Intensification of landfalling typhoons over the northwest Pacific since the late 1970s. *Nature Geoscience*, *9*(10), 753–757. https://doi.org/10.1038/ngeo2792

Menne, M. J., Durre, I., Vose, R. S., Gleason, B. E., & Houston, T. G. (2012). An overview of the global historical climatology network-daily database. *Journal of Atmospheric and Oceanic Technology*, *29*(7), 897–910. https://doi.org/10.1175/JTECH-D-11-00103.1

Murakami, H., Delworth, T. L., Cooke, W. F., Zhao, M., Xiang, B., & Hsu, P.-C. (2020). Detected climatic change in global distribution of tropical cyclones. *Proceedings of the National Academy of Sciences*, *117*(20), 10706–10714. https://doi.org/10.1073/pnas.1922500117

Needham, H. F., Keim, B. D., & Sathiaraj, D. (2015). A review of tropical cyclone-generated storm surges: Global data sources, observations, and impacts. *Reviews of Geophysics*, *53*(2), 545–591. https://doi.org/10.1002/2014RG000477

O'Neill, B. C., Tebaldi, C., Vuuren, D. P. V., Eyring, V., Friedlingstein, P., Hurtt, G., et al. (2016). The Scenario Model Intercomparison Project (ScenarioMIP) for CMIP6. *Geoscientific Model Development*, *9*(9), 3461–3482. https://doi.org/10.5194/gmd-9-3461-2016

Parks, R. M., Anderson, G. B., Nethery, R. C., Navas-Acien, A., Dominici, F., & Kioumourtzoglou, M.-A. (2021). Tropical cyclone exposure is associated with increased hospitalization rates in older adults. *Nature Communications*, *12*(1), 1–12. https://doi.org/10.1038/s41467-021-21777-1

Patricola, C. M., & Wehner, M. F. (2018). Anthropogenic influences on major tropical cyclone events. *Nature*, *563*(7731), 339–346. https://doi.org/10.1038/s41586-018-0673-2

Peduzzi, P., Chatenoux, B., Dao, H., De Bono, A., Herold, C., Kossin, J., et al. (2012). Global trends in tropical cyclone risk. *Nature Climate Change*, *2*(4), 289–294. https://doi.org/10.1038/nclimate1410

Rappaport, E. N. (2014). Fatalities in the United States from Atlantic tropical cyclones: New data and interpretation. *Bulletin of the American Meteorological Society*, *95*(3), 341–346. https://doi.org/10.1175/BAMS-D-12-00074.1

Rayner, N., Parker, D. E., Horton, E., Folland, C. K., Alexander, L. V., Rowell, D., et al. (2003). Global analyses of sea surface temperature, sea ice, and night marine air temperature since the late nineteenth century. *Journal of Geophysical Research*, *108*(D14). https://doi.org/10.1029/2002JD002670

Roberts, M. (2019). *CMIP6 HighResMIP: Tropical storm tracks as calculated by the TempestExtremes algorithm*. Centre for Environmental Data Analysis. Retrieved from https://catalogue.ceda.ac.uk/uuid/438268b75fed4f27988dc02f8a1d756d

Roberts, M. J., Camp, J., Seddon, J., Vidale, P. L., Hodges, K., Vanniere, B., et al. (2020). Impact of model resolution on tropical cyclone simulation using the HighResMIP–PRIMAVERA multimodel ensemble. *Journal of Climate*, *33*(7), 2557–2583. https://doi.org/10.1175/JCLI-D-19-0639.1

Saba, V. S., Griffies, S. M., Anderson, W. G., Winton, M., Alexander, M. A., Delworth, T. L., et al. (2016). Enhanced warming of the Northwest Atlantic Ocean under climate change. *Journal of Geophysical Research: Oceans*, *121*(1), 118–132. https://doi.org/10.1002/2015JC011346

Sobel, A. H., Camargo, S. J., Hall, T. M., Lee, C.-Y., Tippett, M. K., & Wing, A. A. (2016). Human influence on tropical cyclone intensity. *Science*, *353*(6296), 242–246. https://doi.org/10.1126/science.aaf6574

Sutton, R. T., Dong, B., & Gregory, J. M. (2007). Land/sea warming ratio in response to climate change: IPCC AR4 model results and comparison with observations. *Geophysical Research Letters*, *34*(2). https://doi.org/10.1029/2006GL028164

Tang, B., & Camargo, S. J. (2014). Environmental control of tropical cyclones in CMIP5: A ventilation perspective. *Journal of Advances in Modeling Earth Systems*, *6*(1), 115–128. https://doi.org/10.1002/2013MS000294

Ting, M., Camargo, S. J., Li, C., & Kushnir, Y. (2015). Natural and forced north Atlantic hurricane potential intensity change in CMIP5 models. *Journal of Climate*, *28*(10), 3926–3942. https://doi.org/10.1175/JCLI-D-14-00520.1

Ting, M., Kossin, J. P., Camargo, S. J., & Li, C. (2019). Past and future hurricane intensity change along the US East Coast. *Scientific Reports*, *9*(1), 1–8. https://doi.org/10.1038/s41598-019-44252-w

Ullrich, P. A., Zarzycki, C. M., McClenny, E. E., Pinheiro, M. C., Stansfield, A. M., & Reed, K. A. (2021). TempestExtremes v2.1: A community framework for feature detection, tracking and analysis in large datasets. *Geoscientific Model Development Discussions*, *14*, 5023–5048. https://doi.org/10.5194/gmd-14-5023-2021

United Nations. (1982). Convention on the Law of the Sea, Dec. 10, 1982, 1833 U.N.T.S. 397. Retrieved from https://treaties.un.org/doc/Publication/UNTS/Volume%201833/volume-1833-A-31363-English.pdf

Vecchi, G. A., & Soden, B. J. (2007a). Effect of remote sea surface temperature change on tropical cyclone potential intensity. *Nature*, *450*(7172), 1066–1070. https://doi.org/10.1038/nature06423

Vecchi, G. A., & Soden, B. J. (2007b). Increased tropical atlantic wind shear in model projections of global warming. *Geophysical Research Letters*, *34*(8). https://doi.org/10.1029/2006GL028905

Wahl, T., Jain, S., Bender, J., Meyers, S. D., & Luther, M. E. (2015). Increasing risk of compound flooding from storm surge and rainfall for major US cities. *Nature Climate Change*, *5*(12), 1093–1097. https://doi.org/10.1029/2006GL028905

Wang, B., Yang, Y., Ding, Q.-H., Murakami, H., & Huang, F. (2010). Climate control of the global tropical storm days (1965–2008). *Geophysical Research Letters*, *37*(7). https://doi.org/10.1029/2010GL042487

Wang, S., Rashid, T., Throp, H., & Toumi, R. (2020). A shortening of the life cycle of major tropical cyclones. *Geophysical Research Letters*, *47*(14), e2020GL088589. https://doi.org/10.1029/2020GL088589

Wang, S., & Toumi, R. (2021). Recent migration of tropical cyclones toward coasts. *Science*, *371*(6528), 514–517. https://doi.org/10.1126/science.abb9038

Webster, P. J., Holland, G. J., Curry, J. A., & Chang, H.-R. (2005). Changes in tropical cyclone number, duration, and intensity in a warming environment. *Science*, *309*(5742), 1844–1846. https://doi.org/10.1126/science.1116448

Zhu, Y.-J., Collins, J. M., & Klotzbach, P. J. (2021). Nearshore hurricane intensity change and post-landfall dissipation along the United States Gulf and East Coasts. *Geophysical Research Letters*, *48*(17), e2021GL094680. https://doi.org/10.1029/2021GL094680

References From the Supporting Information

Andrews, M. B., Ridley, J. K., Wood, R. A., Andrews, T., Blockley, E. W., Booth, B., et al. (2020). Historical simulations with HadGEM3-GC3.1 for CMIP6. *Journal of Advances in Modeling Earth Systems*, *12*(6), e2019MS001995. https://doi.org/10.1029/2019MS001995

Bi, D., Dix, M., Marsland, S., O'Farrell, S., Sullivan, A., Bodman, R., et al. (2020). Configuration and spin-up of ACCESS-CM2, the new generation Australian Community Climate and Earth System Simulator coupled model. *Journal of Southern Hemisphere Earth Systems Science*, *70*(1), 225–251. https://doi.org/10.1071/ES19040

Boucher, O., Servonnat, J., Albright, A. L., Aumont, O., Balkanski, Y., Bastrikov, V., et al. (2020). Presentation and evaluation of the IPSL-CM6A-LR climate model. *Journal of Advances in Modeling Earth Systems*, *12*(7), e2019MS002010. https://doi.org/10.1029/2019MS002010

Cherchi, A., Fogli, P. G., Lovato, T., Peano, D., Iovino, D., Gualdi, S., et al. (2019). Global mean climate and main patterns of variability in the CMCC-CM2 coupled model. *Journal of Advances in Modeling Earth Systems*, *11*(1), 185–209. https://doi.org/10.1029/2018MS001369

Danabasoglu, G., Lamarque, J.-F., Bacmeister, J., Bailey, D., DuVivier, A., Edwards, J., et al. (2020). The Community Earth System Model Version 2 (CESM2). *Journal of Advances in Modeling Earth Systems*, *12*(2), e2019MS001916. https://doi.org/10.1029/2019MS001916

Döscher, R., Acosta, M., Alessandri, A., Anthoni, P., Arneth, A., Arsouze, T., et al. (2021). The EC-Earth3 Earth system model for the climate model intercomparison project 6. *Geoscientific Model Development*, *15*, 2973–3020. https://doi.org/10.5194/gmd-15-2973-2022

Golaz, J.-C., Caldwell, P. M., Van Roekel, L. P., Petersen, M. R., Tang, Q., Wolfe, J. D., et al. (2019). The DOE E3SM coupled model version 1: Overview and evaluation at standard resolution. *Journal of Advances in Modeling Earth Systems*, *11*(7), 2089–2129. https://doi.org/10.1029/2018MS001603

Gutjahr, O., Putrasahan, D., Lohmann, K., Jungclaus, J. H., von Storch, J.-S., Brüggemann, N., et al. (2019). Max Planck Institute Earth System Model (MPI-ESM1.2) for the high-resolution model intercomparison project (HighResMIP). *Geoscientific Model Development*, *12*(7), 3241–3281. https://doi.org/10.5194/gmd-12-3241-2019

Haarsma, R., Acosta, M., Bakhshi, R., Bretonnière, P.-A., Caron, L.-P., Castrillo, M., et al. (2020). HighResMIP versions of EC-Earth: EC-Earth3P and EC-Earth3P-HR – Description, model computational performance and basic validation. *Geoscientific Model Development*, *13*(8), 3507–3527. https://doi.org/10.5194/gmd-13-3507-2020

Held, I., Guo, H., Adcroft, A., Dunne, J., Horowitz, L., Krasting, J., et al. (2019). Structure and performance of GFDL'S CM4.0 climate model. *Journal of Advances in Modeling Earth Systems*, *11*(11), 3691–3727. https://doi.org/10.1029/2019MS001829

Kelley, M., Schmidt, G. A., Nazarenko, L. S., Bauer, S. E., Ruedy, R., Russell, G. L., et al. (2020). GISS-E2.1: Configurations and climatology. *Journal of Advances in Modeling Earth Systems*, *12*(8), e2019MS002025. https://doi.org/10.1029/2019MS002025

Müller, W. A., Jungclaus, J. H., Mauritsen, T., Baehr, J., Bittner, M., Budich, R., et al. (2018). A higher-resolution version of the Max Planck Institute Earth System Model (MPI-ESM1.2-HR). *Journal of Advances in Modeling Earth Systems*, *10*(7), 1383–1413. https://doi.org/10.1029/2017MS001217

Roberts, M. J., Baker, A., Blockley, E. W., Calvert, D., Coward, A., Hewitt, H. T., et al. (2019). Description of the resolution hierarchy of the global coupled HadGEM3-GC3.1 model as used in CMIP6 HighResMIP experiments. *Geoscientific Model Development*, *12*(12), 4999–5028. https://doi.org/10.5194/gmd-12-4999-2019

Séférian, R., Nabat, P., Michou, M., Saint-Martin, D., Voldoire, A., Colin, J., et al. (2019). Evaluation of CNRM Earth System Model, CNRM-ESM2-1: Role of Earth system processes in present-day and future climate. *Journal of Advances in Modeling Earth Systems*, *11*(12), 4182–4227. https://doi.org/10.1029/2019MS001791

Seland, Ø., Bentsen, M., Olivié, D., Toniazzo, T., Gjermundsen, A., Graff, L. S., et al. (2020). Overview of the Norwegian Earth System Model (NorESM2) and key climate response of CMIP6 DECK, historical, and scenario simulations. *Geoscientific Model Development*, *13*(12), 6165–6200. https://doi.org/10.5194/gmd-13-6165-2020

Sellar, A. A., Jones, C. G., Mulcahy, J. P., Tang, Y., Yool, A., Wiltshire, A., et al. (2019). UKESM1: Description and evaluation of the UK Earth System Model. *Journal of Advances in Modeling Earth Systems*, *11*(12), 4513–4558. https://doi.org/10.1029/2019MS001739

Swart, N. C., Cole, J. N., Kharin, V. V., Lazare, M., Scinocca, J. F., Gillett, N. P., et al. (2019). The Canadian Earth System Model version 5 (CanESM5.0.3). *Geoscientific Model Development*, *12*(11), 4823–4873. https://doi.org/10.5194/gmd-12-4823-2019

Tatebe, H., Ogura, T., Nitta, T., Komuro, Y., Ogochi, K., Takemura, T., et al. (2019). Description and basic evaluation of simulated mean state, internal variability, and climate sensitivity in MIROC6. *Geoscientific Model Development*, *12*(7), 2727–2765. https://doi.org/10.5194/gmd-12-2727-2019

Voldoire, A., Saint-Martin, D., Sénési, S., Decharme, B., Alias, A., Chevallier, M., et al. (2019). Evaluation of CMIP6 DECK experiments with CNRM-CM6-1. *Journal of Advances in Modeling Earth Systems*, *11*(7), 2177–2213. https://doi.org/10.1029/2019MS001683

Volodin, E., & Gritsun, A. (2018). Simulation of observed climate changes in 1850–2014 with climate model INM-CM5. *Earth System Dynamics*, *9*(4), 1235–1242. https://doi.org/10.5194/esd-9-1235-2018

Wu, T., Lu, Y., Fang, Y., Xin, X., Li, L., Li, W., et al. (2019). The Beijing Climate Center Climate System Model (BCC-CSM): The main progress from CMIP5 to CMIP6. *Geoscientific Model Development*, *12*(4), 1573–1600. https://doi.org/10.5194/gmd-12-1573-2019

Wu, T., Zhang, F., Zhang, J., Jie, W., Zhang, Y., Wu, F., et al. (2020). Beijing Climate Center Earth System Model Version 1 (BCC-ESM1): Model description and evaluation of aerosol simulations. *Geoscientific Model Development*, *13*(3), 977–1005. https://doi.org/10.5194/gmd-13-977-2020

Yukimoto, S., Kawai, H., Koshiro, T., Oshima, N., Yoshida, K., Urakawa, S., et al. (2019). The Meteorological Research Institute Earth System Model Version 2.0, MRI-ESM2.0: Description and basic evaluation of the physical component. *Journal of the Meteorological Society of Japan Series II*, *97*(5). https://doi.org/10.2151/jmsj.2019-051

Ziehn, T., Chamberlain, M. A., Law, R. M., Lenton, A., Bodman, R. W., Dix, M., et al. (2020). The Australian Earth system model: ACCESS-ESM1.5. *Journal of Southern Hemisphere Earth Systems Science*, *70*(1), 193–214. https://doi.org/10.1071/ES19035